

Quasi-static analysis of strike fault growth in layered media

Nobuki Kame,¹ Shuji Saito^{1*} and Kenji Oguni²

¹Department of Earth and Planetary Sciences, Faculty of Sciences, Kyushu University, Hakozaki 6-10-1, Higashi-ku, Fukuoka 812-8581, Japan.
E-mail: kame@geo.kyushu-u.ac.jp

²Earthquake Research Institute, University of Tokyo, Yayoi 1-1-1, Bunkyo-ku, Tokyo 113-0032, Japan

Accepted 2007 January 2. Received 2007 November 14; in original form 2007 May 1

SUMMARY

We study the effects of structural inhomogeneity on the quasi-static growth of strike-slip faults. A layered medium is considered, made up of an upper layer bounded by a free surface and welded to a lower half-space with different elastic property. Mode III crack is employed as a mathematical model of strike-slip fault, which is nucleated in the lower half-space and then propagates towards the interface. We adopt FEM- β , newly proposed analysis method for failure, to simulate the quasi-statistic crack growth governed by the stress distribution in layered media. Our results show that along planar traces across interfaces a compliant upper layer has significant effects on promoting/suppressing crack growth before/after its extension into the layer and vice versa for a rigid one. This proposes a possibility that surface breaks due to strike-slip faulting could be arrested by deposit layers at the topmost part of the Earth's crust.

Key words: Numerical solutions; Earthquake dynamics; Dynamics and mechanics of faulting; Fracture and faults; Mechanics, theory and modelling.

1 INTRODUCTION

In theoretical studies of earthquake faulting, rupture propagation has been modelled as growth of cracks in elastic media. Analytic solutions exist only for models that consist of a planar crack in a homogeneous medium (e.g. Kostrov 1966; Husseini *et al.* 1975), though actual earthquakes are generated with non-planar fault geometry in inhomogeneous media. Such complexities are to be tackled by numerical methods. Regarding non-planarity, boundary integral equation methods (BIEM) have been successfully applied to self-chosen faulting path modelling (Kame & Yamashita 1999a,b, 2003; Kame *et al.* 2003; Bhat *et al.* 2004) and have confirmed that non-planar fault geometry has significant effects on earthquake dynamics. Despite of the clear advantage in fault geometry, BIEM analysis is, however, limited to homogeneous media. Finite element method (FEM) and discrete element method (DEM) are major candidates for modelling both non-planar geometry and inhomogeneous medium structure. They are favourable for arbitrary inhomogeneous media because different values of elastic parameters can be described to each element. FEM is ordinarily inadequate for unprescribed crack paths because its smooth and overlapping characteristic function in an element is not suitable for that. On the other hand DEM is suitable for the analysis because failure is easily represented by cutting springs between elements. There, however, remains uncertainty in the equivalence of discrete element model with continuum body. Recently, FEM- β was newly proposed as a method that has advantages of both FEM and DEM (Hori *et al.* 2005), that is, easy treatment

of failure in inhomogeneous continuum body. Here we try to apply FEM- β , originally developed for tensile failure, to shear faulting for the first time.

Our aim here is to investigate the effects of structural inhomogeneity on earthquake faulting. With all the knowledge concerning the significant effect of medium inhomogeneities on seismic wave propagation, it is rather surprising that so little attention has been directed to the effect of medium inhomogeneities on rupture propagation within the Earth. A few examples are Rybicki & Yamashita (1998, 2002), Bonafede *et al.* (2002) and Rivalta *et al.* (2002). This paper is thus intended to be a further step towards this direction. As the simplest model of strike-slip faulting in the Earth's inhomogeneous crust, we consider antiplane (mode III) crack problems in media made up of horizontal layers. A seed crack vertically dipping against horizontal interface is presumed in the deeper half-space, and its quasi-static growth upward is examined. Our main interest is in the possibility of arresting of crack before/after crossing the interface. Rybicki & Yamashita (1998, 2002) have proposed possible arresting mechanisms of rupture in upper compliant layers based on changes in the stress drops and resultant stresses due to layer inhomogeneity. Bonafede *et al.* (2002) have derived integral representations for the stress and displacement fields induced by static cracks with assigned stress drops, located in the proximity of layer discontinuity. However, the shapes and extends of cracks have been given a priori in their analyses and arresting of faulting has not been investigated directly. Here we address this problem by simulating quasi-static crack growth with the aid of FEM- β . It should be noted that due to the presence of inhomogeneous medium structure the stress concentration ahead of crack tip is strongly affected, which influence the process of crack propagation.

*Now at: Hitachi Ltd., Japan.

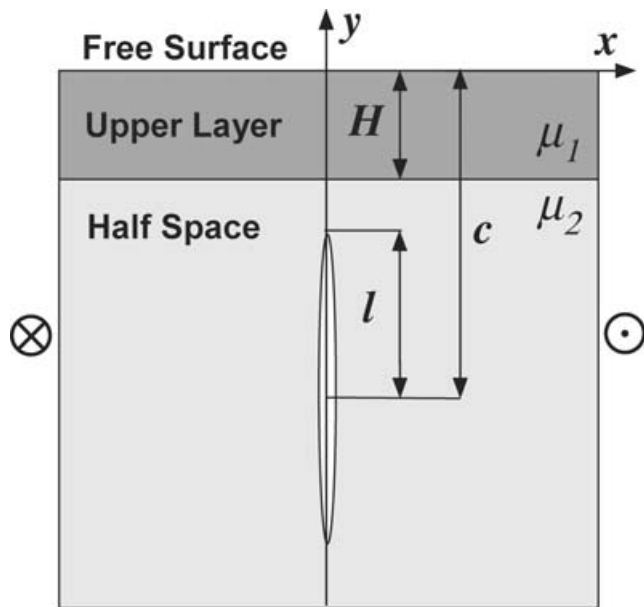


Figure 1. Model configuration. A medium made up of upper elastic layer: $-H \leq y \leq 0$ with rigidity μ_1 , a free surface on $y = 0$ and welded on $y = -H$ to a lower half-space: $y \leq -H$ with elastic parameter μ_2 . A planar seed crack with the half-length l is initially embedded within the half-space and c is its midpoint. Parameters are set to $H = 2.00$ km, $c = 8.00$ km, $l = 5.00$ km, $\mu_2 = 22.5$ GPa. A compliant layer $\mu_1/\mu_2 = 1/10$ for ‘model A’, and a rigid layer $\mu_1/\mu_2 = 10$ for ‘model B’ are assumed.

2 MODEL AND METHOD

2.1 Crack in layered medium

Configuration of our model is shown in Fig. 1. It is the same as in Bonafede *et al.* (2002). An antiplane deformation is considered, in which the only non-vanishing component of the displacement field is $u_z(x, y)$, which is independent of the coordinate z . The medium consists of an upper layer that is bounded by a free surface and welded along its base to a half-space with different rigidity and a mode III crack is employed as a model for strike-slip fault. A seed crack is initially assumed in the half-space and quasi-static growth from this is examined. In this paper, two opposite cases are considered for the rigidity ratio of the upper layer μ_1 to the lower μ_2 : ‘model A’ for a compliant case with $\mu_1/\mu_2 = 1/10$ [the same ratio as employed in Bonafede *et al.* (2002)] and ‘model B’ for a rigid case with $\mu_1/\mu_2 = 10$ (adopted here for comparison). Remotely applied stresses of $\sigma_{xz}^0 = 5.00 \times 10^{-1}$ MPa, 5.00×10^1 MPa, and 5.00 MPa are considered in the upper layers of model A, model B and the lower half-spaces, respectively. Shear stresses are assumed to be completely released on crack surfaces and thus a stress-drop discontinuity condition, $\Delta\sigma_1/\Delta\sigma_2 = \mu_1/\mu_2$, is satisfied on cracks if they extend across interfaces with planar traces. The material interface is kept welded for such intersecting cracks under this condition (Bonafede *et al.* 2002; Rybicki & Yamashita 2002). Accordingly planar paths without fracturing the interface are possible in our simulation.

2.2 Implementation of crack growth by FEM- β

FEM- β is very facilitative for the analysis of crack propagation: ordinary FEM requires intensive mesh adaptation while FEM- β does not require any special treatment. It solves a boundary value problem of a continuum body by applying Voronoi block particle dis-

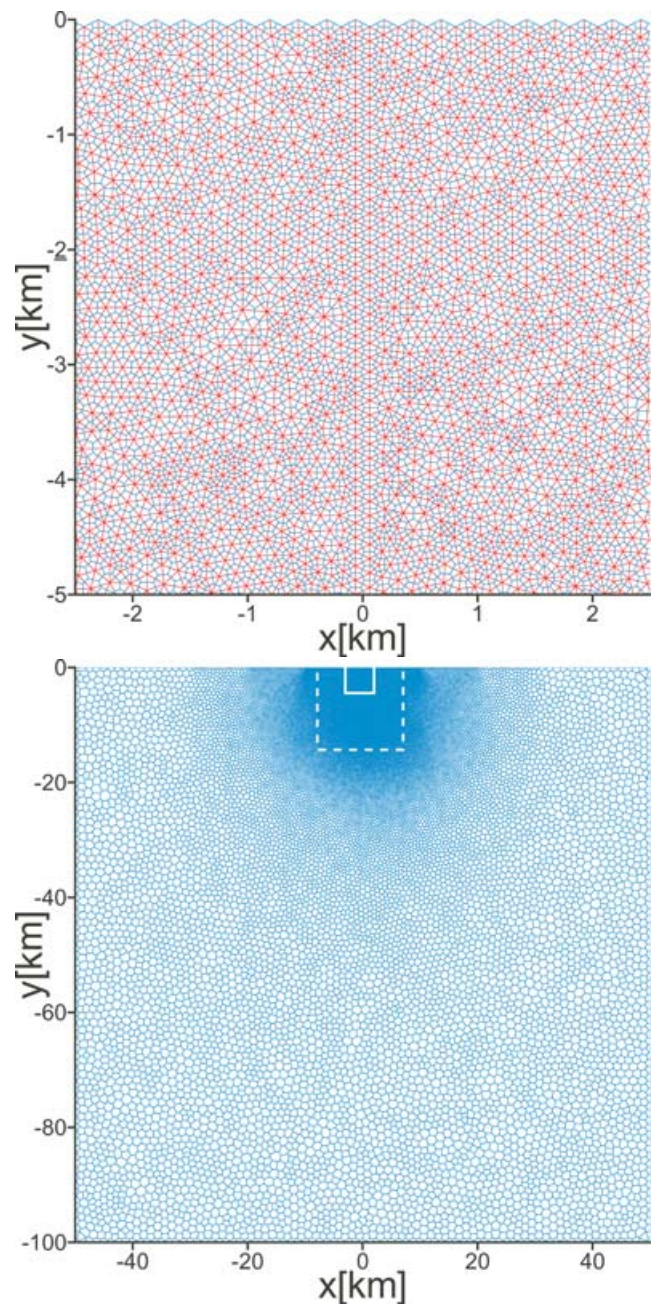


Figure 2. (a) Mesh configuration: close view ($|x| \leq 2.5$ km, $-5 \leq y \leq 0$ km) in the vicinity of the interface. Voronoi blocks (blue lines) and Delaunay triangles (red lines) are distributed at even intervals along the seed crack, layer interface, and free surface within the part of our interest ($|x| \leq 7.5$ km, $-15 \leq y \leq 0$ km). Separation of any two adjacent Voronoi block is possible in FEM- β analysis. (b) Mesh configuration of the whole domain ($|x| \leq 50$ km, $-100 \leq y \leq 0$ km). It totally consists of 30 892 blocks (blue lines) and 61 257 triangles (not plotted for brevity). Solid and dashed lines indicate regions for the close view and the part of our interest, respectively.

cretization and the conjugate Delaunay tessellations to displacement and stress fields, respectively (Fig. 2a). The key point of FEM- β is the ease of expressing failure as separation of two adjacent Voronoi blocks owing to the particle discretization that uses non-overlapping characteristic functions, and results from FEM- β is more reliable than that from DEM in the sense that equivalence to the continuum is assured in FEM- β . It is shown that a solution of FEM- β has the

same accuracy as that of ordinary FEM with triangular elements (Hori *et al.* 2005). Note that separated blocks no longer sustain any shear stresses and thus residual stresses such as friction can not be assigned in FEM- β in the present form because it is originally aimed for tensile failure.

Whole mesh configuration employed in our simulation is shown in Fig. 2(b). A finite 100×100 km rectangular domain is discretized as an approximation of infinite layered medium and our interest is concentrated in a much smaller part of 15×15 km² within which the stress fields are plotted hereafter. In order to attain the remotely applied stresses, we impose a fixed displacement boundary condition on the two vertical edges of the whole domain that gives a uniform strain of $\epsilon_{xz}^0 = 1.11 \times 10^{-4}$ if there is no crack. This realizes a nearly constant stress loading stated above, over the part of interest throughout the crack growth. A planar seed crack with initial length l is first introduced in the half-space and the stress distribution is computed. The quasi-static growth of crack upward is then simulated from this state.

Prior to simulation, we first corroborate FEM- β accuracy by comparing the numerical solution with analytic one for a mode III crack. In unbounded homogeneous medium, analytic solution is available in a simple algebraic form (e.g. Pollard & Segall 1987). Fig. 3 shows a detailed comparison of stress changes in $\Delta\sigma_{xz}$ component along the crack plane. For the FEM- β solution, mesh is arranged as fine as in Fig. 2: only exception is that the finer mesh part is centred on the whole domain. Both our stress distribution and the analytical one fit with each other very well except for two points outside the crack tip. The computation errors are 4 and 1 per cent for the first and second points, respectively. Note that this range of errors is precise enough for the present analysis and does not make a significant difference in our conclusions. Fig. 4 shows comparison of the stress changes $\Delta\sigma_{xz}$ in layered medium. It also shows good quantitative agreement both in space and in magnitude.

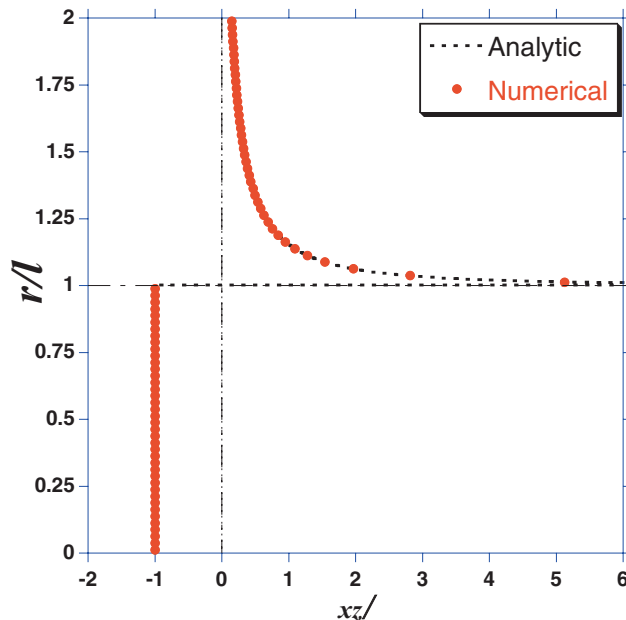


Figure 3. Comparison between analytical solution (broken line) and FEM- β computation (dots) for stress changes $\Delta\sigma_{xz}$ along a crack plane in homogeneous medium, where position r is measured from the centre of crack. r and $\Delta\sigma_{xz}$ are normalized by the crack half-length l and the assigned stress drop $\Delta\sigma$, respectively.

For a fracture criterion, we adopt a simple criterion of strength-of-material type as in Hori *et al.* (2005). In FEM- β simulation, if a triangular element has the maximum shear stress $\tau_{\max}(\vec{n}) = \sigma_{xz}n_x + \sigma_{yz}n_y$ that reaches threshold strengths τ_{ci} ($i = 1, 2$ for upper layers and half-spaces, respectively), a Voronoi block interface whose normal vector is closest to the maximum direction \vec{n} is broken. This criterion is similar to that often used in the DEM simulations and the only difference is the usage of the maximum stress as an indicator of fracture; force applied to the spring is used in DEM. It is often a problem that stress evaluated numerically at the tip is strongly dependent on the dimensions of elements because of the singularity (e.g. Fig. 3). When the element spacing is fixed, however, the simple strength criterion is approximately equivalent to the stress intensity factor based criterion (Das & Aki 1977). In order to validate the simple strength criterion, we employ an almost identical spacing for elements inside the part of our interest (Fig. 2a). We search all the elements in it for the largest $\tau_{\max}(\vec{n})$ throughout simulation. It enables us not to miss unnoticed non-planar failure paths across the boundaries though planar paths are sufficiently possible under the stress discontinuity condition.

The material strength over the half-space is set to τ_{c2} that is slightly smaller than the largest τ_{\max} value locating just above the upper tip of the seed crack. In the simulation, the stress distribution is recomputed after the crack extension for the same boundary condition and another interface to be broken is found. This process is repeated until τ_{\max} no longer reaches τ_{ci} . As well as the rigidity ratio μ_1/μ_2 , the strength ratio τ_{c1}/τ_{c2} also affects the whole failure processes as will be shown in the following section.

3 RESULTS

Fig. 5 shows snap shots of the crack growth with the corresponding σ_{xz} stress field in model A with a compliant upper layer, $\mu_1/\mu_2 = 1/10$. Clear stress gaps are identified across the interface: strain ϵ_{xz} must be continuous across it because of the ‘welded’ condition during the crack growth and stresses just above it are thus discontinuously reduced to $1/10$ due to the rigidity contrast. Being proceeded by the largest $\tau_{\max}(\vec{n})$ element, the crack path initially extends straight in the half-space until the tip touches the interface. If τ_c is uniform over the whole domain (denoted as ‘stress case’ with $\tau_{c1}/\tau_{c2} = 1$), the crack will be arrested there at the interface $y = -2.00$ km. In order for the crack to propagate further we here tentatively assume that the strength of compliant layer τ_{c1} is simply reduced to $\tau_{c1} = (1/10)\tau_{c2}$, so that the ratio of τ_{c1}/τ_{c2} is the same as μ_1/μ_2 . It means that the same critical strain is assumed as a fracture criterion over the domain (‘strain case’). Then the crack continues to grow upward in a straight way and finally penetrates the layer up to the surface.

Fig. 6(a) shows τ_{\max} evolution with the crack growth, that is, the peak stresses reached before failure at each position. For convenience, the stresses and strengths are plotted with a magnification of 10 within the compliant layer. In model A, there occurs significant increases of τ_{\max} towards the interface and surface. These can be attribute to the so-called mirror effect with respect to a free surface: stress enhancement against a free surface due to a mode III crack is equivalently modelled by two symmetrically distributed cracks with respect to the virtual surface in an unbounded body. The interface in model A affects as a kind of free surface due to the more compliant layer and this contributes to the first peak. After crossing the interface, the mirror source effect with respect to it vanishes and τ_{\max} decreases accordingly. As the crack tip approaches the true

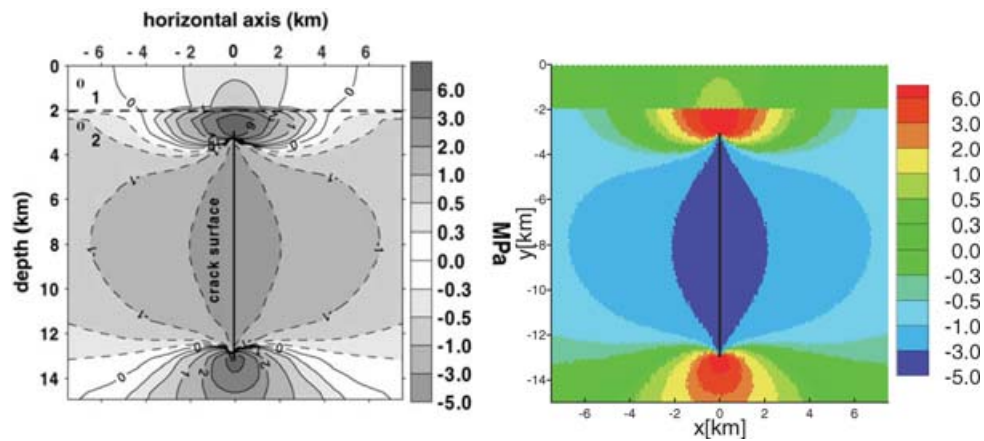


Figure 4. Comparison between analytic integral representation (left-hand side) (after Bonafede *et al.* 2002) and FEM- β computation (right-hand side) for the stress changes $\Delta\sigma_{xz}$ induced by a crack with stress drop $\Delta\sigma = 5.00$ MPa in layered medium.

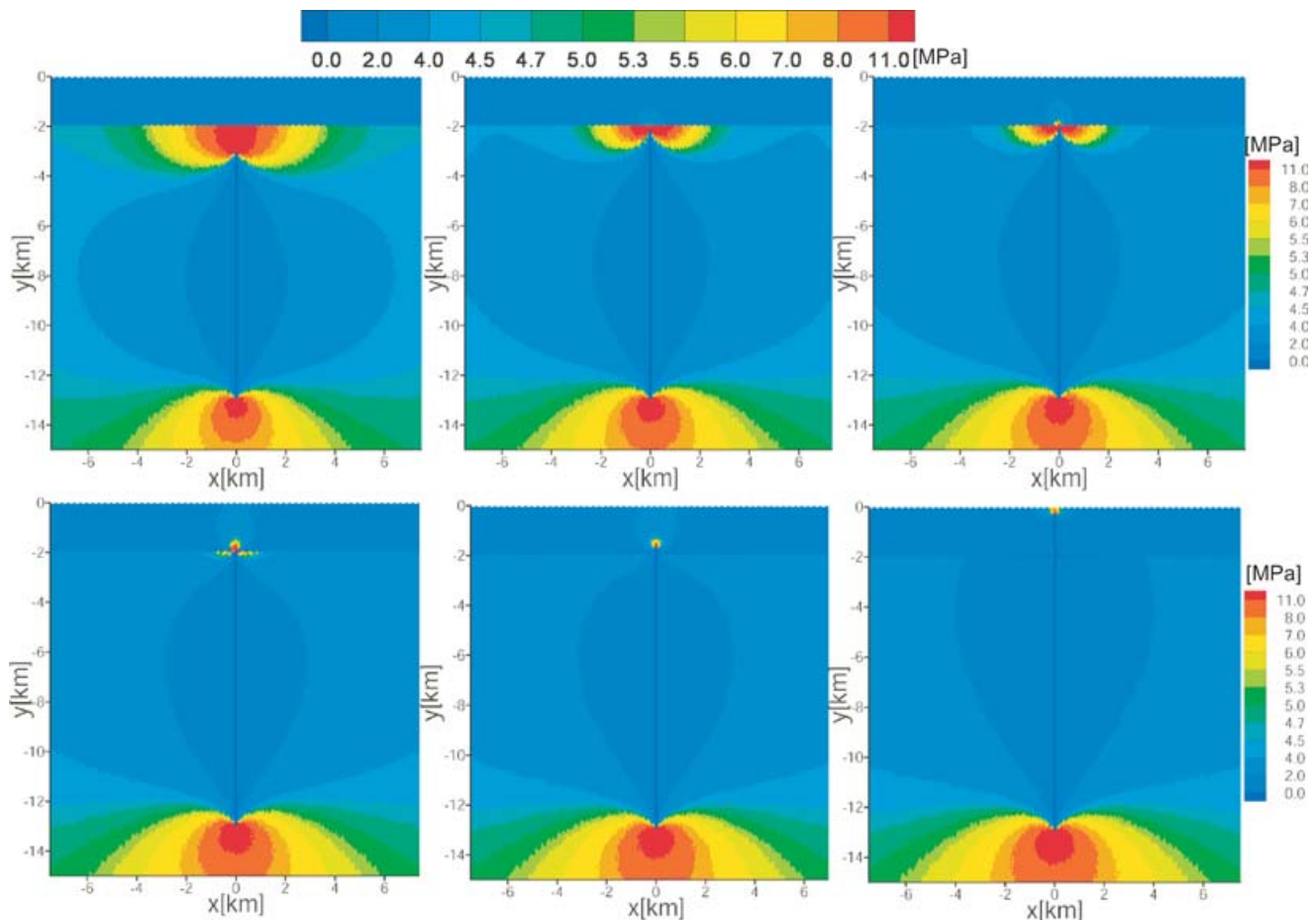


Figure 5. Snap shots of crack growth in model A ($\mu_1/\mu_2 = 1/10$ and $\tau_{cz} = 59.9$ MPa) with the corresponding σ_{xz} stress field. Upper crack tip locations are $y = -3.00, -2.13$ and -2.00 km from left- to right-hand side in the upper row and $y = -1.88, -1.63$ and -0.25 km in the lower row, respectively.

surface, another mirror effect emerges and τ_{\max} again increases significantly. τ_{\max} in the upper layer takes the minimum 13.3 MPa at $y = -0.82$ km. This means that if we assume τ_{c1} as an intermediate value between the minimum and the ‘stress case’ strength, the crack growth is arrested in the compliant layer (‘intermediate case’). It should be noted that three cases of τ_{c1} assumed here are totally suppositional: we do not have any experimental data on rocks that show clear dependency of strength on the rigidity. However, τ_{c1} assump-

tion between the two specific cases of ‘stress’ and ‘strain’ seems acceptable and realistic to rocks in the Earth’s crust.

Finally we examine crack growth in model B with a rigid upper layer, $\mu_1/\mu_2 = 10$. In this model, τ_{\max} decreases with the first extension of the tip, that is, the crack does not propagate quasi-statically. For clarification of the effect of a rigid layer, we here force the crack to extend up to the surface choosing the largest $\tau_{\max}(\vec{n})$ element even if it does not reach τ_{ci} . Our simulation again shows that

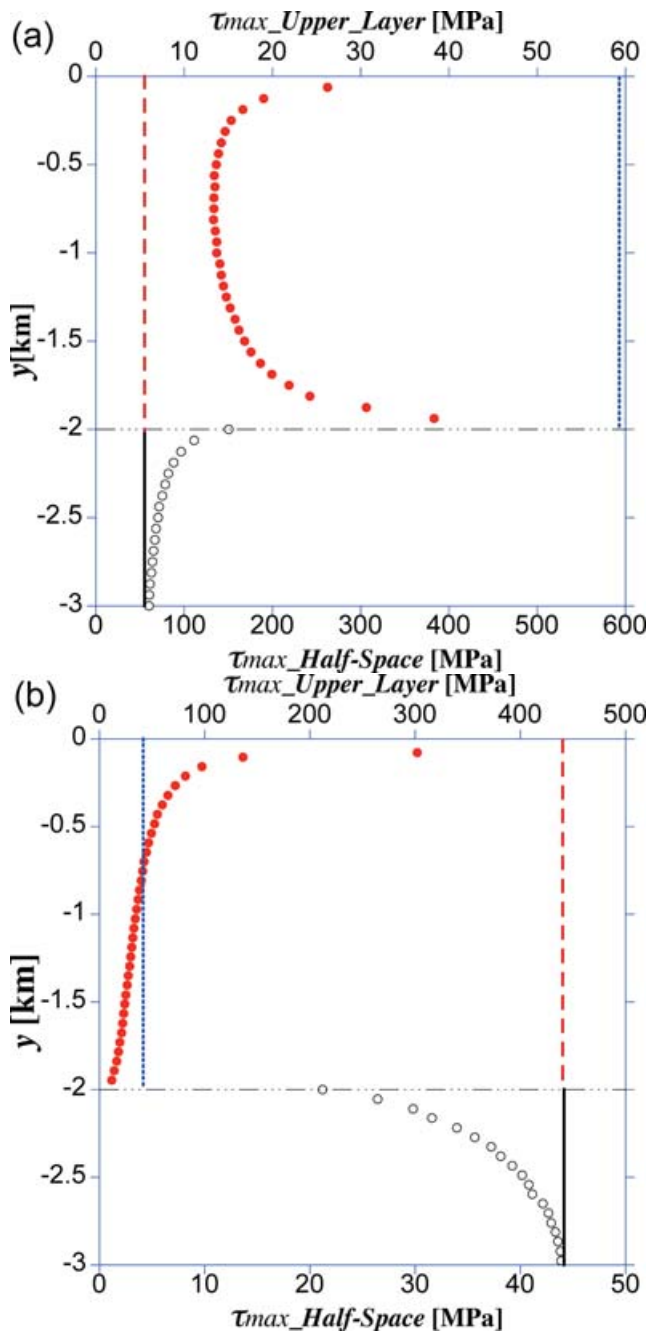


Figure 6. (a) τ_{\max} evolution with the quasi-static crack growth in model A ($\mu_1/\mu_2 = 1/10$). $\tau_{c2} = 59.9$ MPa is plotted with a solid line in the half-space. In the upper layer, the strengths for ‘stress case’ ($\tau_{c1}/\tau_{c2} = 1$: dotted line) and for ‘strain case’ ($\tau_{c1}/\tau_{c2} = 1/10$: dashed line) are plotted for reference. (b) τ_{\max} evolution with the compulsory crack extension in model B ($\mu_1/\mu_2 = 10$). $\tau_{c2} = 44.8$ MPa is plotted with a solid line on the half-space. The strengths for ‘stress case’ ($\tau_{c1}/\tau_{c2} = 1$: dotted line) and for ‘strain case’ ($\tau_{c1}/\tau_{c2} = 10$: dashed line) are also plotted. Note that all the quantities within the upper layers are plotted with magnification of 10 (model A) and 1/10 (model B), respectively.

totally planar crack path is chosen in model B. The resulting τ_{\max} evolution accompanied with such compulsive extension is plotted in Fig. 6(b) with a magnification of 1/10 in the rigid upper layer this time. A significant decrease of τ_{\max} appears towards the interface. This is because the deformation in the half-space is prevented by

the upper rigid layer. After prolongation of the crack into the upper layer, the stresses turn to increase: the stresses are enhanced by the larger stress drop in the rigid layer ($\Delta\sigma_1/\Delta\sigma_2 = 10$) and by the mirror source effect towards the free surface. Relative relationship between the two speculative types of strength ($\tau_{c1}/\tau_{c2} = 10$ for ‘strain case’ and $\tau_{c1}/\tau_{c2} = 1$ for ‘stress case’) indicates that the ‘strain case’ becomes more difficult for a surface break than the ‘stress case’ and this is quite contrary to model A.

4 DISCUSSION AND CONCLUSIONS

We investigated the effects of structural inhomogeneity on the growth of strike-slip faults, considering a model that consists of a mode III crack in a layered medium. With facilitative use of FEM- β we simulated successfully the quasi-statistic crack growth governed by stress distribution in the layered medium. Our results directly showed that totally planar crack paths are formed across layer boundaries quasi-statically under the stress drop discontinuity condition ($\Delta\sigma_1/\Delta\sigma_2 = \mu_1/\mu_2$), which has not been straightforwardly shown in the pioneer analyses of faulting in layered media (Rybicki & Yamashita 1998, 2002; Bonafede *et al.* 2002). And we clearly demonstrated that a compliant upper layer has significant effects on promoting/suppressing crack growth before/after extension into the layer and vice versa for a rigid one. The effect of structural inhomogeneity ($\mu_1/\mu_2 < 1$) on strike-slip faulting suggests the possibility that the surface break is prohibited under specific (and realistic) assumptions related to medium strength τ_c , with a strike-slip fault being arrested in upper deposit layers. Our simulation results support quantitatively the possible arresting mechanism of earthquake rupture due to a compliant upper layer proposed by Rybicki & Yamashita (1998, 2002).

We may note that the existence of compliant upper layers of thickness of few kilometres, located above mode rigid lower bedrock is known to take place frequently in the Earth’s crust. However, the rigidity contrast assumed in model A is not realistic from the point of view of available data related to medium structure: the value of rigidity contrast about 1/2 is much more realistic (Ben-Zion *et al.* 1992). We thus tested an additional case with the ratio $\mu_1/\mu_2 = 1/2$: τ_{\max} evolution with the planar crack growth shows the same tendency as in Fig. 6(a): it first increases, then reduces beyond the interface and takes the minimum at $y = -1.19$ km in the upper compliant layer. Finally it turns to increase towards the free surface. The minimum τ_{\max} again becomes smaller than the ‘stress case’ and larger than the ‘strain case’ as same as in model A. This means that our conclusions are valid for the more realistic case.

As the first step in applying FEM- β to earthquake shear faulting, we have concentrated the cases for which the stress-drop discontinuity condition is satisfied. Otherwise (e.g. inhomogeneous initial strains across interfaces) the welded interface state are not guaranteed and thus there raises a possibility that crack fails to keep its planarity as pointed out by Bonafede *et al.* (2002). Such process does affect the arresting of rupture propagation and is to be investigated in further studies by FEM- β . Non-planar crack growth is also expected dynamically even under the stress drop discontinuity condition (Kame & Yamashita 1999a). Such possibility is also to be examined by dynamic version of FEM- β .

ACKNOWLEDGMENTS

This research was supported by the Earthquake Research Institute cooperative research program, Japan.

REFERENCES

- Ben-Zion, Y., Katz, S. & Leary P., 1992. Joint inversion of fault zone head waves and direct P arrivals for crustal structure near major faults, *J. geophys. Res.*, **97**(B2), 1943–1951.
- Bhat, H.S., Dmowska, R., Rice, J.R. & Kame, N., 2004. Dynamic slip transfer from the Denali to Totschunda faults, Alaska: testing theory for fault branching, *Bull. seism. Soc. Am.*, **94**, 202–213.
- Bonafede, M., Parenti, B. & Rivata, E., 2002. On strike-slip faulting in layered media, *Geophys. J. Int.*, **149**, 698–723.
- Das, S. & Aki, K., 1977. A numerical study of two-dimensional spontaneous rupture propagation, *Geophys. J. R. astr. Soc.*, **50**, 643–668.
- Hori, M., Oguni, K. & Sakaguchi, H., 2005. Proposal of FEM implemented with particle discretization for analysis of failure phenomena, *J. Mech. Phys. Solids*, **53**, 681–703.
- Husseini, M.I., Jovanovich, D.B., Randall, M.J. & Freund, L.B., 1975. The fracture energy of earthquakes, *Geophys. J. R. astr. Soc.*, **43**, 367–385.
- Kame, N. & Yamashita, T., 1999a. Simulation of the spontaneous growth of a dynamic crack without constraints on the crack tip path, *Geophys. J. Int.*, **139**, 345–358.
- Kame, N. & Yamashita, T., 1999b. A new light on arresting mechanism of dynamic earthquake faulting, *Geophys. Res. Lett.*, **26**, 1997–2000.
- Kame, N. & Yamashita, T., 2003. Dynamic branching, arresting of rupture and the seismic wave radiation in a self-chosen crack path modelling, *Geophys. J. Int.*, **155**, 1042–1050.
- Kame, N., Rice, J.R. & Dmowska, R., 2003. Effects of pre-stress state and rupture velocity on dynamic fault branching, *J. geophys. Res.*, **108**(B5), 2265, doi:10.1029/2002JB002189.
- Kostrov, B.V., 1966. Unsteady propagation of longitudinal shear cracks, *J. Appl. Math. Mech.*, **30**, 1241–1248.
- Pollard, D.D. & Segall, P., 1987. Theoretical displacements and stresses near fractures in rock: with applications to faults, joints, veins, dikes, and solution surfaces, in *Fracture Mechanics of Rock*, pp. 277–349, ed. Atkinson, B.K., Academic Press, London.
- Rivalta, E., Mangiavillano, W. & Bonafede, M., 2002. The edge dislocation problem in a layered elastic medium, *Geophys. J. Int.*, **149**(2), 508–523.
- Rybicki, K.R. & Yamashita, T., 1998. Faulting in vertically inhomogeneous media and its geophysical implications, *Geophys. Res. Lett.*, **25**(5), 2893–2896.
- Rybicki, K.R. & Yamashita, T., 2002. On faulting in inhomogeneous media, *Geophys. Res. Lett.*, **29**(10), doi:10.1029/2002GL014672.